Journal of Hydroscience and Hydraulic Engineering
Vol. 21, No.2 November, 2003, 93-102

NUMERICAL ANALYSIS OF ACCELERATING TURBIDITY THERMALS

By

Toshihiko Eto

Graduate School, Nagaoka Univ. of Tech., Nagaoka, Niigata 940-2188, Japan

and

Yusuke Fukushima

Dept. of Civil and Environ. Engrng, Nagaoka Univ. of Tech., Nagaoka, Niigata 940-2188, Japan

SYNOPSIS

Turbidity thermals are numerically analyzed using the $k-\varepsilon$ turbulence model. The basic equations are discretized by the implicit method and the pressure equation is solved by the SIMPLE method. The constants in the $k-\varepsilon$ turbulence model are set to be the standard values. Turbidity thermals are generated when sediment covering the bed of a channel is eroded by turbulence of saline thermals. Calculations were carried out for the following 5 cases: i.e. cases of four grain sizes and a case of no sediment. One of these cases shows that the turbidity thermal can erode the sediment layer and accelerate in the flow direction; thus, that is the ignition condition for the accelerating turbidity thermal. The variations of travel speed, maximum height, maximum concentration and contours of concentration and velocity vectors of turbidity thermals are obtained and compared with the results of saline thermals. The characteristics of accelerating turbidity thermals are remarkably different from the other cases.

INTRODUCTION

A turbid gravity current is observed on slopes in the ocean or in deep lakes when bed sediment is entrained by turbulent motion or sometimes by wave action (refer to Inman *et al* (12); Parker (13)). This temporary or intermittent phenomenon is a kind of non-conservative inclined thermal because the total negative buoyancy is changed by deposition or suspension of sediment. The total negative buoyancy decreases when the deposition dominates, and it increases when the bed sediment is entrained by water. In the latter, the thermal grows and accelerates with time and distance. Fig. 1 shows the schematic view of a non-conservative thermal on a constant slope.

Parker (13) studied accelerating turbidity currents analytically under the conditions that the layer thickness does not change and that the steady flow is established. He has found that the turbidity current can accelerate itself when some hydraulic condition is satisfying. He called such a condition the "ignition condition." Fukushima and Parker (7) studied the flow characteristics of steady turbidity currents which accelerate or decelerate, based on the

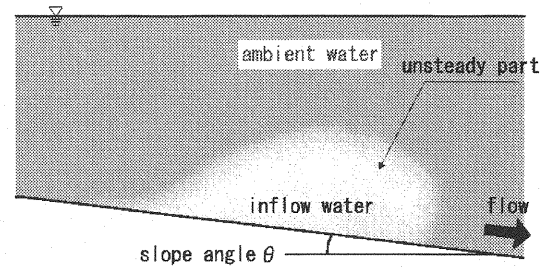

Fig.1 Schematic view of turbidity thermals

idea of the ignition condition. They analyzed turbidity currents numerically using the layer integral equations and applied the method to the Scripps Submarine Canyon. Parker *et al.* (14) and Garcia (11) carried out laboratory experiments on steady turbidity currents such as plumes in order to confirm the idea of the ignition condition. Eto and Fukushima (3), (5) analyzed steady turbidity currents on a constant slope to get the profiles of velocity and sediment concentration, which were compared with previous experimental results. Eto and Fukushima (4) analyzed conservative inclined thermals with the slope angle of 30° using the k-ε turbulence model in order to examine their flow characteristics. Eto and Fukushima (6) also analyzed non-conservative inclined thermals with the slope angles of 10° and 30° composed of water and barium sulfate particles using the k-ε turbulence model.

In this study, flow characteristics of a turbidity thermal on a constant slope are numerically analyzed by using the $k-\varepsilon$ model. The effect of bed sediment condition on the flow pattern, especially its difference between an accelerating thermal and a decelerating one, is focused to clarify the "ignition condition" which has been discussed in previous studies. In the calculation, some simplifications are made; the thermal is initiated artificially by a high salinity water mass placed on the upstream end of the slope; the slope is covered by uniform non-cohesive sediment; the bed topography is not changed by erosion or deposition; and the grain size is the only one parameter which is varied in the calculation. These simplifications are to illuminate the basic mechanism which separates accelerating thermals from decelerating ones and help us to understand the effects of erosion or deposition of bed sediment on the flow characteristics of thermals.

NUMERICAL MODEL OF INCLINED THERMAL

Consider a flow of a turbidity thermal on a constant slope. The coordinate system is depicted in Fig. 2. The fresh water with the uniform density ρ_w is filled in a two-dimensional tank with the bed slope angle θ. The saline water of the constant concentration c_s, and the density ρ_s starts to flow from the upstream of the channel. The bed of the slope is covered with sediment of uniform grain size and of density ρ_p. These sediments are eroded by the flow of a saline thermal. It is assumed that the volume of eroded sediment is not so large and that the deformation of the bed form is small. The method of numerical analysis is essentially the same as that used in Eto and Fukushima (4). Thus, the mass conservation equation for mixture, the Reynolds equations in x and z directions, the equations of kinetic energy of turbulence k and the viscous dissipation rate of turbulence ε are used as the basic equations. In this study, the diffusion equations for salinity and sediment particles are added to describe their transport by a thermal. The diffusion equation for salinity is the same as that used in Eto and Fukushima (4). The transport of sediment particles are expressed by the diffusion equation that considers the

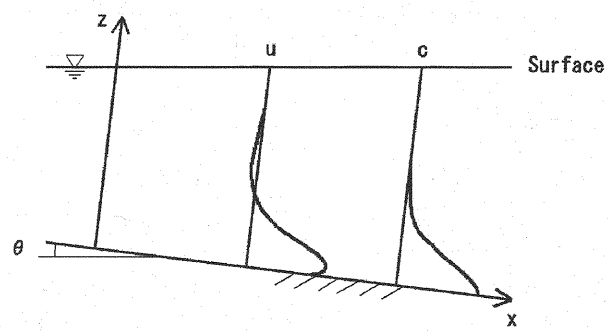

Fig.2 Coordinate system for numerical calculation

Table.1 Calculational conditions

salinity c_0(%)	density of saline water ρ_s(g/cm^3)	density of fresh water ρ_w(g/cm^3)	relative density difference $\Delta\rho/\rho_w$	density of sediment ρ_p(g/cm^3)	diameter of sediment D_s(mm)
5	1.043105	0.999220	0.043885	2.65	0.028 to 0.031

deposition and erosion of turbid materials. These equations are as follows:

(1)The diffusion equation for salinity

$$\frac{\partial c_s}{\partial t}+u\frac{\partial c_s}{\partial x}+w\frac{\partial c_s}{\partial z}=D\left(\frac{\partial^2 c_s}{\partial x^2}+\frac{\partial^2 c_s}{\partial z^2}\right)+\frac{\partial}{\partial x}\left(\frac{\nu_t}{\sigma_t}\frac{\partial c_s}{\partial x}\right)+\frac{\partial}{\partial z}\left(\frac{\nu_t}{\sigma_t}\frac{\partial c_s}{\partial z}\right) \tag{1}$$

(2)The diffusion equation for the sediment particles

$$\frac{\partial c_p}{\partial t}+(u+w_s\sin\theta)\frac{\partial c_p}{\partial x}+(w-w_s\cos\theta)\frac{\partial c_p}{\partial z}$$
$$=D\left(\frac{\partial^2 c_p}{\partial x^2}+\frac{\partial^2 c_p}{\partial z^2}\right)+\frac{\partial}{\partial x}\left(\frac{\nu_t}{\sigma_t}\frac{\partial c_p}{\partial x}\right)+\frac{\partial}{\partial z}\left(\frac{\nu_t}{\sigma_t}\frac{\partial c_p}{\partial z}\right) \tag{2}$$

where c_p is the volume concentration of sediment particles, u and w are the velocity components of x and z direction, w_s is the settling velocity of sediment particles in still water, D is the molecular diffusion coefficient. ν_t is the eddy viscosity defined by $\nu_t=c_\mu k^2/\varepsilon$, in which σ_t and c_μ are numerical constants in the k-ε turbulence model. The density of the mixture of saline water and sediment particles, ρ, is expressed as follows:

$$\rho=\rho_0(1+R_g c_p) \tag{3}$$

$$\rho_0=\rho_w(1+R_s c_s) \tag{4}$$

where ρ_0 is the density of saline water, $R_s c_s$ is the relative density difference of saline water in which $R_g c_p(=(\rho_p-\rho_0)/\rho_0)$ is the relative density difference of turbid water composed of saline water and sediments. The above basic equations are discretized using the SIMPLE method proposed by Patankar (15).

Erosion or deposition can occur connected with the motion of a thermal. In order to express this mechanism, the following equation is adopted as the boundary condition at the bottom of particles. At $z=z_0$,

$$-\frac{\nu_t}{\sigma_t}\frac{\partial c_p}{\partial z}=w_s E_s \tag{5}$$

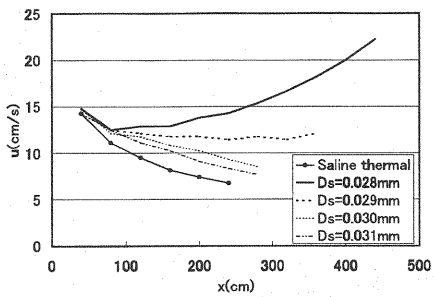

Fig.3 Travel speed.

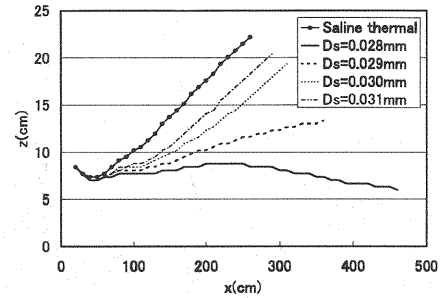

Fig.4 Maximum thickness.

where E_s is the sand entrainment coefficient. The functional form of the sand entrainment equation is determined by Garcia (11) who used many experimental data of open channel suspension flows, as follows:

$$E_s = AZ_u^5 \Big/ \left(1 + \frac{A}{0.3} Z_u^5\right) \qquad (6)$$

$$Z_u = R_p^{0.6} u_* / w_s \qquad (7)$$

$$R_p = \sqrt{gR_g D_s} D_s / \nu \qquad (8)$$

where $A = 1.3 \times 10^{-7}$, D_s is the diameter of sand particle, u_* is the firction velocity at the bottom. This equation (6) is sensitively changed with the value of Z_u, for example, $E_s = 1.3 \times 10^{-7}$, when $Z_u = 1$ and $E_s = 1.25 \times 10^{-2}$, when $Z_u = 10$. Thus, the function E_s has the threshold value which will change with the diameter of sediments.

NUMERICAL ANALYSIS OF INCLINED THERMALS AND DISCUSSIONS

The calculational conditions of the numerical analysis are summarized in Table 1. The calculational domain is 500cm in x direction and 94.2cm in z direction with the slope angle of $\theta = 10°$. Initial water depth is 5.96cm at the upstream end and 94.2cm at the downstream end. It is assumed that the saline water of the initial concentration 5% was filled in the trapezoid area at $x = 0$ to 10cm at the upstream end in the initial stage. The remaining part of the tank is filled with fresh water of density ρ_w. The numerical calculation was carried out until t = 30s with the time step $\Delta t = 0.1$s. The saline water started to flow because of the density difference between saline water and fresh water and forms a thermal. The saline thermal eroded and suspended sediment particles from the bed. Calculations have been carried out for the following 5 cases: i.e. the grain size of the particles is $D_s = 0.028$mm, 0.029mm, 0.030mm, 0.031mm, respectively, and the saline thermal with no particles. The grain size is decided as the range which includes both cases of accelerating and decelerating turbidity currents. The travel speed and the maximum thickness of a thermal were obtained on the basis of the saline concentration contour. The mass of suspended particles in water is defined by the weight of sediments. The flow characteristics of a thermal are dependent upon the grain size of particles. The concentration contours and velocity vectors of salinity thermals and particle thermals will be shown later. The concentration profiles of particles in a thermal are also obtained. The results of saline thermals are almost the same as those presented by authors (Eto and Fukushima (4)).

The travel speed of inclined thermals is shown in Fig. 3. The inclined thermals decelerate in all cases until $x = 100$cm. At the downstream of $x = 100$cm, in the case of $D_s = 0.029$mm, the travel speed is nearly constant; In the case of $D_s = 0.028$mm, the travel speed increases, i.e. a turbidity thermal accelerates. The mechanism of these flows is considered as follows. The mass of particles in a thermal increases when the erosion of particles

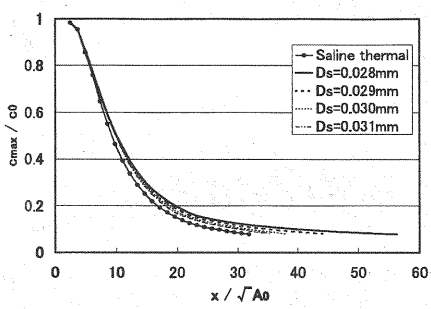

Fig.5 Maximum salinity concentration.

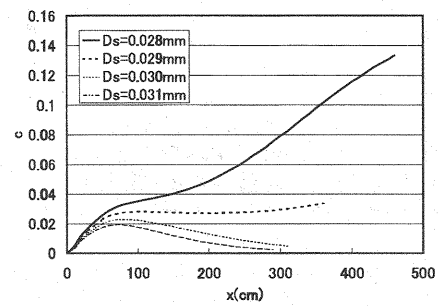

Fig.6 Maximum sediment concentration.

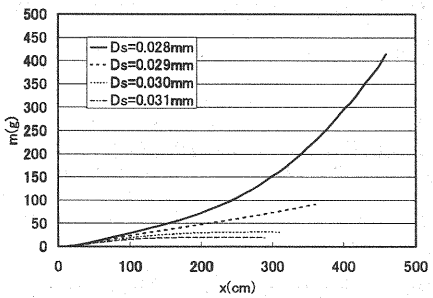

Fig.7 Weight of sediment particles.

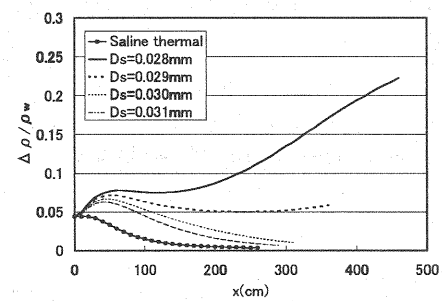

Fig.8 Maximum relative density difference.

from the bed dominates the deposition of particles. Thus a turbidity thermal can accelerate by itself. The maximum thickness of inclined thermals is shown in Fig. 4. The larger the grain size is, the larger the maximum thickness is. The maximum thickness decreases after x = 200cm in the case of D_s = 0.028mm. In the other cases, the maximum thickness linearly increases in the flow direction. In the case of small grain size, the sediment concentration increases near the bed. Therefore, the velocity vector to flow direction increases near the bed, and the spread of salinity concentration to z direction is controlled. The maximum salinity concentration of inclined thermals is shown in Fig. 5. The travel distance x is non-dimensionalized using the square root of the initial area A of saline water; thus, the horizontal axis is non-dimensionalized as $x/\sqrt{A}$. The maximum salinity concentration c_{max} is non-dimensionalized by the initial salinity concentration c_0 as the vertical axis. The difference of the variation of maximum salinity concentration is not so large in all cases. The maximum concentration decreases gradually just after a quick decrease at the initial stage. Thus, the variation of maximum salinity concentration in the non-dimensional form is almost the same, although the amount of the erosion of sediment varies greatly. In other words, the entrainment of ambient water is almost the same in all cases. The maximum sediment concentration of inclined thermals is shown in Fig. 6. In cases of D_s = 0.030mm and 0.031mm, the maximum concentration decreases because the fall velocity of particles is large. The maximum concentration is shown to be nearly a constant in the case of D_s = 0.029mm. It increases remarkably at the downstream of x = 100cm in the case of D_s = 0.028mm. The weight of sediment in inclined thermals is shown in Fig. 7. The weight of sediment increases in all cases. The smaller the grain size of particles is, the larger the weight of sediment is. The variation of maximum relative density difference is shown in Fig. 8. In cases of the saline thermal, D_s = 0.030mm and D_s = 0.031mm, the maximum relative density differences decrease in the flow direction. It is almost a constant in the case of D_s = 0.029mm. On the contrary, it increases remarkably in the case of D_s = 0.028mm.

In order to clarify the inner structure of thermals, the salinity concentration contours, the sediment con-

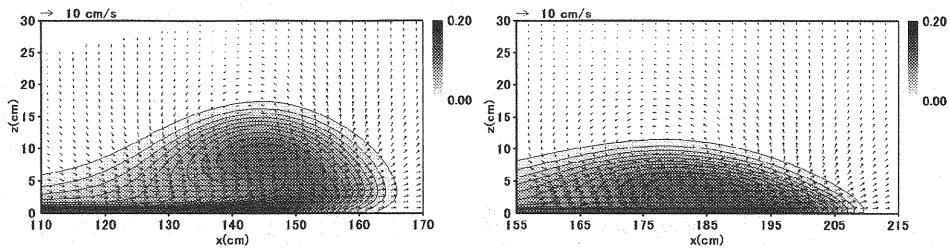

Fig.9 Velocity vectors and salinity concentration contours (left: saline, right: Ds=0.028mm) t=15s.

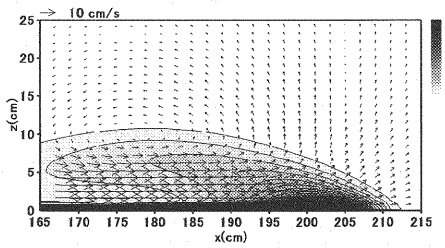

Fig.10 Velocity vectors and sediment concentration contours (D_s=0.028) t=15s.

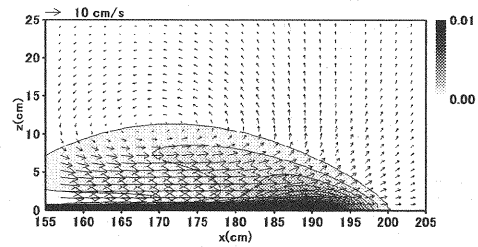

Fig.11 Velocity vectors and sediment concentration contours (D_s=0.029) t=15s.

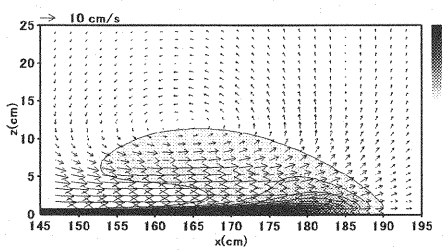

Fig.12 Velocity vectors and sediment concentration contours (D_s=0.030) t=15s.

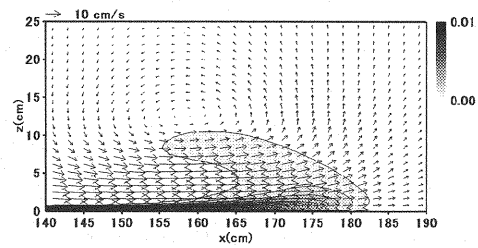

Fig.13 Velocity vectors and sediment concentration contours (D_s=0.031) t=15s.

centration contours and the velocity vectors are shown in Fig. 9 to Fig. 13. The velocity vectors and salinity concentration contours in the case of the saline thermal and D_s = 0.028mm at t = 15s are shown in Fig. 9. The shape of a thermal is a half ellipse in these cases. A large-scale circulation forms around the thermal. In the case of D_s = 0.028mm, the maximum thickness is smaller than that of the saline thermal and its shape is totally flat. The velocity vectors near the bed become larger and the concentration contours in the z direction become flat due to the effect of the erosion of sediment particles from the bed.

The velocity vectors and sediment concentration contours in the cases of D_s = 0.028mm, D_s = 0.029mm, D_s = 0.030mm and D_s = 0.031mm at t = 15s are shown in Fig. 10 to Fig. 13, respectively. In the case of D_s = 0.030mm and D_s = 0.031mm, the sediment concentration contours are considerably different from the salinity concentration contours; that is, the shapes of saline thermals and accelerating turbidity thermals are apparently different. In the case of D_s = 0.028mm and D_s = 0.029mm, the shapes of sediment thermals are relatively similar to those of saline thermals. The sediment concentration of these cases is much larger than that in the cases of D_s = 0.030mm and D_s = 0.031mm. The position of the center of circulation around the thermal is low in the cases of small grain size.

The velocity vectors and the sediment concentration contours in the case of D_s = 0.028mm, whose case shows strong acceleration, are shown in Fig. 14, and the elapsed times are t = 10s, 20s and 30s, respectively. An

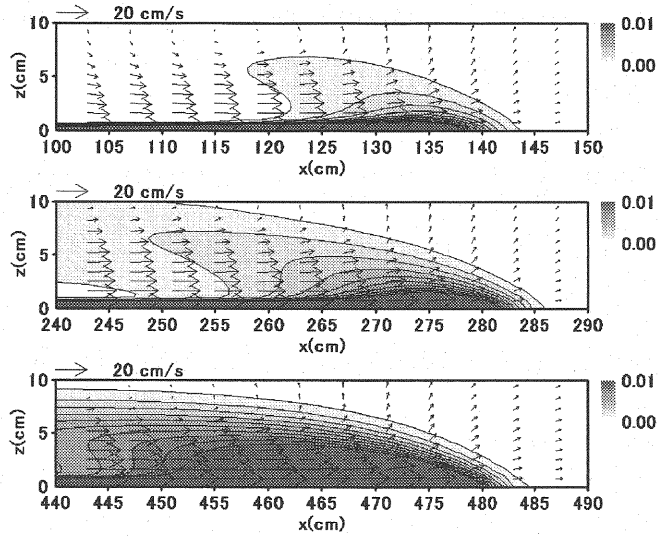

Fig.14 Velocity vectors and sediment concentration contours (D_s=0.028mm) t=10s, 20s and 30s.

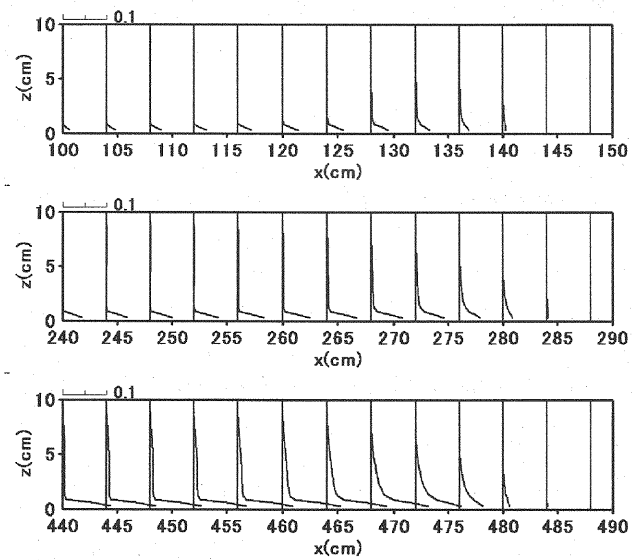

Fig.15 Profile of sediment concentration (D_s=0.028mm) t=10s, 20s and 30s.

examination of these figures indicates that the sediment concentration tends to increase and that the thermal tends to develop with the elapsed time. In this case, the concentration of sediment increases rapidly and the sediment spreads extensively. In addition, the velocity vectors near the bottom increase with the elapsed time.

The sediment concentration contours and profiles in the case of D_s = 0.028mm are shown in Fig. 15. The elapsed times are 10s, 20s and 30s from the top, respectively, as shown in Fig. 15. These figures show that the sediment concentration near the bottom increases and the sediment concentration spreads to the upper region. This sediment concentration profiles are appreciably different from the salinity concentration profiles of saline plumes (Fukushima (9)). They are similar to the profiles of sediment of the open channel suspension or the concentration profiles of snowdrifts (Fukushima et al. (10)).

The process by which the saline thermal erodes and suspends the sediments near the bed and develops into the turbidity thermal is analyzed. Several new findings are described above. The equation proposed by Garcia (11) is used in this paper as the sand entrainment coefficient. This relationship was obtained from the concentration profiles of suspended sediment in the open channel flow. There are some problems in applying this relation to turbidity currents, so further investigation is needed. The calculational results are totally varied, according to the small difference of grain size. Therefore, the flow characteristics of turbidity currents in the case of mixed sediments should also be investigated. It should be noted that the deformation of configuration of the bed is not considered in this study. This effect should be taken into account in the case of the large erosion of sediment.

Although some problems are pointed out in the present model, the findings obtained from our investigations are very important. Begin et al. (2) reported the experimental results with the wide range of the slope angle. As a result, they show that the shape of thermals is almost similar in the same slope angle, i.e. semi-elliptical shape. The shape of thermals in the cases of slight erosion and deposition of sediment is similar to the conservative one (Eto and Fukushima (4)). On the contrary, the shape of thermals in the accelerating case changes significantly in the flow direction. They are not similar in the flow direction. From this point of view, this effect should be taken into account in the simulation model of non-conservative inclined thermals accelerating in the flow direction, for example, powder snow avalanches.

CONCLUSION

The numerical calculation was carried out using the k-ε turbulence model to clarify the mechanism of accelerating turbidity thermals. The SIMPLE method proposed by Patankar (15) was used to discretize partial differential equations. Numerical constants in the k-ε turbulence model were used as the standard values. The calculation was carried out under the condition that the saline thermal was generated at the upstream end and the turbulence eroded the sediment particles from the bed. Five flow conditions were considered, i.e. the four different grain size and no sediment. The travel speed, the maximum thickness of saline thermal and other flow properties were obtained from the numerical calculations and were shown in figures. The flow characteristics of sediment cases were different from the saline case. The concentration contours of salinity and the velocity vectors were obtained from the numerical results. It was found that the shape of the accelerating turbidity thermal was remarkably different from the other cases. The concentration contours, the velocity vectors and the profiles of sediment particle concentration were obtained in the sediment cases. It should be pointed out that sediment concentration contours and the salinity concentration contours were completely different. The profiles of sediment concentration were similar to those of open channel suspension flows or snowdrifts(Fukushima(8), Fukushima et al.(10)).

Part of this study was supported by Grant-in-Aid for Scientific Research (C)(Grant number 13650565; Chief Researcher Yusuke Fukushima) by the Japanese Ministry of Education, Science, Sport and Culture. The authors express their appreciation.

REFERENCES

1. Akiyama, J. and Y. Fukushima: Entrainment of non-cohesive bed sediment into suspension, St. Anthony Falls Hydraulic Lab., Univ. of Minnesota, External Memorandum, No.195, p.33, 1985.

2. Beghin, P., E.J. Hopfinger and R.H. Britter: Gravitational convection from instantaneous sources on inclined boundaries, Jour. Fluid Mech., 107, pp.407-422, 1981.

3. Eto, T. and Y. Fukushima: Analysis of turbidity currents in submarine canyon using the $k-\varepsilon$ turbulence model, Jour. Japanese Coastal Engineering, Vol.48, pp.461-465, 2001.

4. Eto, T. and Y. Fukushima: Numerical analysis of conservative inclined thermals using k-ε turbulence model, Annual Journal of Hydraulic Engineering, JSCE, Vol.46, pp.1043-1048, 2002a.

5. Eto, T. and Y. Fukushima: Numerical Analysis of Turbidity Currents Using k-ε Turbulence Model, Advances in Fluid Modeling and Turbulence Measurements, editors H. Ninokata, A. Wada and N. Tanaka, IAHR, pp.331-338, 2002b.

6. Eto, T. and Y. Fukushima: Analysis of unsteady turbidity currents using k-ε turbulence model, Jour. Japanese Coastal Engineering, JSCE, Vol.49, pp.446-450, 2002c.

7. Fukushima, Y. and G. Parker: Study on self-accelerating turbidity currents, Proc. 32nd Conference on Coastal Engineering, JSCE, Vol.32, pp.253-257, 1985.

8. Fukushima, Y.: Analysis of turbulent structure of open-channel flow with suspended sediments, Annual Journal of Hydraulic Engineering, JSCE, Vol.30, pp.631-636, 1986.

9. Fukushima, Y.: Analysis of inclined wall plume by turbulence model, Proc. Japan Society of Civil Engineers, No.399/II-10, pp.65-74, 1988.

10. Fukushima, Y., T. Eto, S. Ishiguro, K. Kosugi and T. Sato: Flow analysis of developing snowdrifts using a $k-\varepsilon$ turbulence model, Seppyo (Jour. Japanese Soc. of Snow and Ice), Vol.63, pp.373-383, 2001.

11. Garcia, M.: Depositing and eroding sediment driven flows: turbidity currents, St. Anthony Falls Hydraulic Lab., Univ. of Minnesota, Project Report, 306, p.179, 1990.

12. Inman, D. L., C.E. Nordstrom and R.E. Flick: Currents in submarine canyons : an air-sea-land interaction, Annual Rev. of Fluid Mech., 8, pp.275-310. 1976.

13. Parker, G.: Condition for the ignition of catastrophically erosive turbidity currents, Marine Geology, 46, pp.307-327, 1982.

14. Parker, G., M. Garcia, Y. Fukushima and W. Yu: Self-accelerating turbidity currents, Journal of Fluid Mechanics, 171, pp.145-182, 1987.

15. Patankar, S. V.: Numerical Heat Transfer and Fluid Flow, Hemisphere Pub. Co., 1980.

APPENDIX — NOTATION

The following symbols are used in this paper:

$c_{1\varepsilon}$ = numerical constant in the $k-\varepsilon$ turbulence model;

$c_{2\varepsilon}$ = numerical constant in the $k-\varepsilon$ turbulence model;

$c_{3\varepsilon}$ = numerical constant in the $k-\varepsilon$ turbulence model;

c_p = volume concentration of the sediment particles;

c_s = salinity concentration;

c_μ = numerical constant in the $k-\varepsilon$ turbulence model;

D = molecular diffusion coefficient;

D_s = diameter of sediment;

E_s = sand entrainment coefficient;

g = gravitational acceleration;

k = kinetic energy of turbulence;

p = pressure;

R_s = specific weight of sediment in water;

R_g = specific weight of saline water in water;

t = time;

u = velocity component of x direction;

u_* = shear velocity at the bottom;

w = velocity component of z direction;

w_s = settling velocity of the sediment particles;

x = coordinate in the flow direction;

z = coordinate in the direction perpendicular to the x direction;

ε = viscous dissipation rate of turbulence;

θ = slope angle;

ν_t = eddy viscosity;

ρ = density of the mixture of the saline water and the sediment particles;

ρ_0 = density of saline water;

ρ_p = density of sediment particles;

ρ_s = density of saline water;

ρ_w = density of fresh water;

σ_t = Schmidt number of turbulence.

(Received June 11, 2003 ; revised September 12, 2003)